Analytica Chimica Acta 1101 (2020) 111–119

Contents lists available at ScienceDirect

Analytica Chimica Acta

journal homepage: www.elsevier.com/locate/aca

Enzyme induced molecularly imprinted polymer on SERS substrate for ultrasensitive detection of patulin

Yuanyuan Zhu [a, 1], Long Wu [a, 1], Heng Yan [b], Zhicheng Lu [a], Wenmin Yin [a], Heyou Han [a, *]

[a] State Key Laboratory of Agricultural Microbiology, College of Science, Huazhong Agricultural University, Wuhan, Hubei, 430070, PR China
[b] Hubei Provincial Engineering and Technology Research Center for Food Quality and Safety Test, Hubei Provincial Institute for Food Supervision and Test, Wuhan, Hubei, 430075, PR China

HIGHLIGHTS

- A new type of MIP-SERS substrate which combined the selectivity of molecular imprinting polymer (MIP) and the sensitivity of SERS technology was prepared with uniform structure and dense "hot spots".
- The method behaved a wide linear range of 5×10^{-10} to 10^{-6} M with limit of detection of 8.5×10^{-11} M.
- The MIP-SERS substrate can be easily used without complex sample pretreatment.

GRAPHICAL ABSTRACT

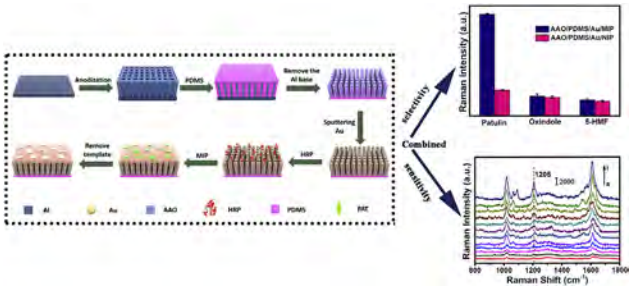

ARTICLE INFO

Article history:
Received 24 July 2019
Received in revised form
6 December 2019
Accepted 11 December 2019
Available online 13 December 2019

Keywords:
Surface-enhanced Raman spectroscopy
Molecular imprinting polymer
Free-radical polymerization
Patulin
Au/PDMS/AAO substrate

ABSTRACT

We designed a new type of MIP-SERS substrate for specific and label-free detection of patulin (PAT), by combining molecular imprinting polymer (MIP) selectivity and SERS technology sensitivity. Initially, the solid substrate of PDMS/AAO was prepared using poly dimethylsiloxane (PDMS) concreted anodized aluminum oxide (AAO) template. Then moderate Au was sputtered on the surface of PDMS/AAO to obtain Au/PDMS/AAO SERS substrate. Based on the HRP enzyme initiated in situ polymerization on the Au/PDMS/AAO, the MIP-SERS substrate was successfully synthesized with selective polymer and high tense of SERS "hot spots". The new MIP-SERS substrate showed strong SERS enhancement effect and good selectivity for PAT. Besides, the results showed that the method owned a linear range from 5×10^{-10} to 10^{-6} M with the limit of detection (LOD) of 8.5×10^{-11} M (S/N = 3) for PAT. The proposed method also exhibited acceptable reproducibility (relative standard deviation, RSD = 4.7%) , good stability (Raman intensity is above 80% after two weeks) and recoveries from 96.43% to 112.83% with the average RSD of 6.3%. The substrate is easy to use without complex sample pretreatment, which makes it a potential candidate as a rapid and sensitive detection method in food samples.

1. Introduction

With the progress and development of society and the people's living standard improvement, progressively more citizens are concerned about the quality and food safety. Among many food contaminants, the natural toxin produced by fungi in the food can

* Corresponding author.
E-mail address: hyhan@mail.hzau.edu.cn (H. Han).
[1] Equal contribution.

https://doi.org/10.1016/j.aca.2019.12.030
0003-2670/

cause potential health risks to humans. Wherein, PAT, one of the common natural toxins, is commonly found in fruits (apples, hawthorn, etc) or nuts (almonds, peanuts, hazelnuts, etc) [1]. Studies reported that patulin could make acute and chronic poisoning impact on human's body, including convulsions, lung, liver and intestinal bleeding, kidney damage or neurotoxicity, immunotoxicity, teratogenicity, and possible carcinogenicity [2,3], which may be ascribed to the toxicity of hemiacetal and lactone rings [4].

Due to the high risks of PAT in food, different countries and organizations have formulated the maximum limit of PAT. For example, the European Union has proposed that the maximum permissible limits of PAT in children and baby food are 10 μg kg^{-1} (9.86×10^{-8} M) [5]. Maximum limits (MLs) of PAT for fruit juice and fruit products are 50 μg kg^{-1} (4.93×10^{-7} M) adopted by Codex Alimentarius Commission [6]. The same limits were abided by the Food and Drug Administration (FDA) and China [7]. Thus, the potential threat of PAT and its related contamination have been a global problem. Therefore, establishing a rapid and sensitive method to monitor PAT is extremely urgent.

Usually, the analytical techniques for PAT are chromatographic methods such as thin layer chromatography (TLC) [8,9], gas chromatography (GC) [10], high performance liquid chromatography (HPLC) [11,12] and gas chromatography-mass spectrometry (GC-MS) [13,14]. Moreover, immunoassay has also received intensive attention because of their specificity and simplicity [15]. For example, immunoassay combined with fluorescence surface plasmon resonance (FSPR), quartz crystal microbalance, and chemiluminescence are widely used for the detection of PAT [16–18]. All the above methods have their advantages, but also have the shortcoming of troublesome pretreatment, low separation degree and sensitivity, high price and/or low repeatability. Hence, it is of great significance to construct comprehensive method by proposing new strategy for PAT detection.

Surface-enhanced Raman spectroscopy (SERS), a promising analytical tool in food safety and life science, has the advantages of high sensitivity, rich molecular information, and narrow peak band [19]. When the nano-gap between the two nanoparticles is less than 10 nm, the resonance local electromagnetic field generated by the plasma excitation is greatly enhanced, and the region is usually called a hot spot. Therefore, weak Raman scattering can be amplified to generate SERS signals of analytes located in these hot-spots, then achieve sensitive detection [20,21]. However, control over the gap distance between NPs in colloids is still challenging, which makes it problematic to use SERS for quantitative detection. Furthermore, this has become the subject of intensive research [22–25]. Besides, due to SERS poor selectivity restriction [26], identification and aggregation targets rapidly in complex samples are still considered a tough work for SERS.

Molecular imprinting technique (MIT) is a different approach to produce synthetic receptors, which have the sites for specific recognition in synthetic polymers [27–29]. It has the advantages of high selectivity, good predictability and versatility [30–32]. Because of this, many studies have combined the specific recognition properties of MIP and the signal amplification properties of SERS to solve the limitations of SERS [33–36]. Inspired by this, a new type of MIP-SERS substrate was prepared in our work for the selective and sensitive detection of PAT by uniting MIP and SERS technique together which was easy to use without complex sample pretreatment, had excellent selectivity and sensitivity for PAT, and exhibited acceptable reproducibility and good stability.

Attributable to the good moldability, high elasticity, and adhesion properties, PDMS had broad application prospects in the fields of surface-enhanced Raman spectroscopy [37,38], microfluidics [39,40], and biochips [41,42]. In this work, the MIP-SERS substrate was prepared by using AAO as template, afterward PDMS was solidified on AAO surface to form a flexible transparent elastomeric polymer. Next, aluminum matrix was removed using copper chloride solution to obtain PDMS/AAO nanoarrays. After sputtering with gold nanoparticles, HRP was immobilized on this film surface. Then PAT was used as template, 4-VP as functional monomers, PDA as cross-linker, and the free radical polymerization was initiated by HRP. As shown in Scheme 1, the new MIP-SERS substrate possessed flexible mechanical properties and excellent SERS performance. Besides, the SERS substrate is easy to operate without complex sample pretreatment, which makes it a promising method in the rapid and sensitive detection in food samples.

2. Materials and methods

2.1. Chemicals and materials

5-Hydroxymethylfurfural (5-HMF, 95%), 1,4-Diacryloylpiperazine (PDA, 97%), oxindole (98%), 4-vinyl pyridine (4-VP, 95%), horseradish peroxidase (HRP, 180U) were purchased from Aladdin Chemistry Co., Ltd.; Patulin (PAT, 95%) standard (PAT, > 99.0%) was supplied by Dr Ehrenstorfer (Augsburg, Germany); SYLGARD 184 Silicone Elasomer Base and SYLGARD 184 Silicone Elastomer Curing Agent were obtained from Dow Corning Corporation. Ultra-pure aluminum (99.999%) was purchased from Alfa Aesar; Phosphoric acid (H_3PO_4), chromium oxide (Cr_2O_3), absolute ethanol (C_2H_5OH), methanol (CH_3OH), acetic acid, acetylacetone, hydrogen peroxide (H_2O_2, 30%) and ammonium hydroxide ($NH_3 \cdot H_2O$, 25%) were offered by Sinopharm Chemical Reagent. All aqueous solutions were prepared with ultrapure water (18.2MΩ resistivity).

2.2. Instruments

Raman tests were conducted by an inVia Raman spectrometer (Renishaw, U.K.) equipped with a confocal microscope (Leica, Germany). The Raman spectra were scanned under the following conditions: a diode laser at 785nm, laser power 0.05 W, acquisition time 10 s. UV–vis absorption spectra were measured by PerkinElmer LAMBDA 25 (PerkinElmer, UK). Fourier-transform infrared (FT-IR) spectra were obtained from a Nicolet Avatar-330 spectrometer. Transmission electron microscopy (TEM) images were acquired by transmission electron microscopy (TEM, JEM-2010). The Dynamic Light Scattering was measured with a Zeta-sizer Nano ZS90 DLS system (Malvern, England). NGSLabSpec and Origin 8.5 were used for statistical calculations and graphical displays.

2.3. Fabrication of Au/PDMS/AAO nanoarray

Before the preparation of Au/PDMS/AAO nanoarray, AAO and PDMS/AAO were first prepared according to the previously reported method [43]. Then, we used the pure aluminum sheets to fabricate the AAO template by two-step anodization [44,45]. The detailed procedures of Au/PDMS/ AAO substrate were described in Supporting Information.

2.4. Preparation of MIP-ir-Au/PDMS/AAO

MIP-ir-Au/PDMS/AAO (MIP-SERS) substrate was prepared by the following two steps: (1) immobilize horseradish peroxidase (HRP) on Au/PDMS/AAO substrate and (2) induce polymerization reaction on the substrate surface. Firstly, the appropriate amount of Au/PDMS/AAO was incubated with 50 mM PBS buffer (pH = 7.0) solution containing 2 mg HRP for 12 h at room temperature. Through the physical and chemical force [46], HRP can be immobilized on the surface of Au/PDMS/AAO substrate. After that, the substrate was

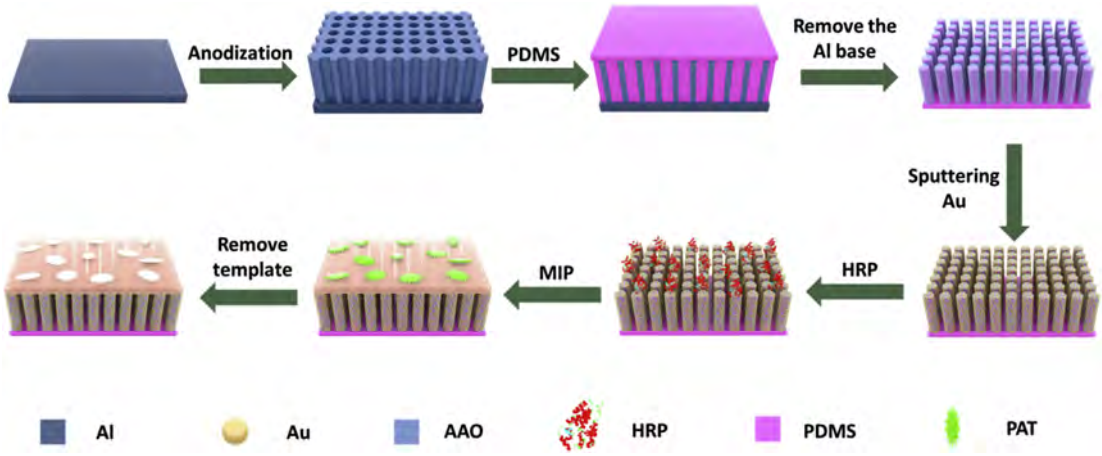

Scheme 1. Illustration of the preparation process of enzyme induced MIP-SERS substrate (MIP-ir-Au/PDMS/AAO).

then rinsed three times with washing buffer to remove the free HRP, and the HRP-Au/PDMS/AAO complex was obtained and stored at 4 °C in PBS buffer.

The polymerization process on HRP-Au/PDMS/AAO complex was carried out according to Attieh' s method [47]. To be specific, 4-VP (0.58 mM) acted as functional monomer, PDA (2.32 mM) as cross-linker and PAT (0.1 mM) as a template, which was mixed to prepare the molecularly imprinted polymer. The above mixture was placed in a glass tube capped with an airtight septum, then HRP-Au/PDMS/AAO were introduced. After that, acetylacetone (0.035 mM) was added in a bottle and kept in ice by bubbling nitrogen for 10 min. Finally, 200 μL hydrogen peroxide (0.1 M) was introduced to the mixture and kept for 3 days at 25 °C under gentle agitation. Finally, the PAT imprinted Au/PDMS/AAO (MIP-SERS) substrates were obtained.

To remove the PAT template, the MIP-SERS substrates were washed 3 times by incubating in methanol/acetic acid (v:v, 8:2), methanol/acetic acid (v:v, 9:1), methanol and acetonitrile. A non-imprinted polymer of NIP-ir-Au/PDMS/AAO (NIP-SERS) was prepared following the same way but without PAT template. Then the MIP-SERS and NIP-SERS substrates were dried in vacuum and stored at 4 °C refrigerator.

2.5. Detection methods

Before the SERS tests, MIP-SERS and NIP-SERS substrates were incubated with PAT concentrations from 10^{-12} to 10^{-5} M and from 10^{-10} to 10^{-4} M, respectively. And then, the substrates were taken out and cleaned with purified water to remove the free PAT. Next, the MIP-SERS and NIP-SERS substrates were dried at room temperature. Finally, the prepared substrates were measured by the Raman spectrometer.

2.6. Selectivity studies

To estimate the selectivity of MIP-SERS, 100 μL of PAT, oxindole and 5-HMF were mixed with MIP-SERS substrate, respectively. Then the mixture was shaken in a washed glass at 4 °C for 2 h. Finally, the MIP-SERS substrate was taken out and washed with water for the Raman measurements.

2.7. Detection of real samples

Unlike other analytical methods, the proposed MIP-SERS method does not require pretreatment. Basically, 1 g of blueberry jam, grapefruit jam and orange juice were incubated with MIP-SERS substrate for 1 h, respectively. Then the real samples packaged on the substrate surface were removed by purified water. After that, the samples can be detected by Raman spectrometer under optimal conditions.

3. Results and discussion

3.1. Characterization of MIP-SERS substrate

SEM images for the synthetic composites are shown in Fig. 1. It can be seen in Fig. 1A that each hole of AAO is well-aligned and the side-view illustrated that the depth of the unique nanoarchitecture is about 500 nm. As depicted in Fig. 1B, the obtained AAO/PDMS membrane is of high uniformity with nanosized gaps. Followed that, Au was sputtered on the AAO/PDMS surface to make a flexible SERS substrate. As shown in Fig. 1C, the top-view of Au/PDMS/AAO exhibited uniform Au nanoflower with a great deal of "hot spots" [48–50], which could help the substrate produce huge SERS enhancement. Based on the Au/PDMS/AAO substrate, the PAT imprinted polymer was synthesized as displayed in Fig. 1D. A thin polymer membrane was covered on the Au/PDMS/AAO substrate, which remained the morphology of the SERS substrate. Through X-ray photoelectron spectroscopy (XPS), we could find that the element peak of N appeared on the Au/PDMS/AAO substrate after coating the polymer in Fig. S1, and the result was consistent with Fig. 1D.

Moreover, the size of the AAO hole and the sputtering time of Au/PDMS/AAO were explored and characterized. To discuss the pore size distribution of AAO, phosphoric acid was adopted to enlarge the holes. The SEM images of AAO under different treatment times were displayed in Fig. S2. It showed that the hole of AAO enlarged with the increasing of treatment time (Fig. S2A-**C**). When the time is 40 min or longer, the edge of the hole appears damaged (Figs. S2D–F). To obtain large and uniform holes as much as possible, 30 min was chosen as the optimal time. Besides, the distance between the two pores is closest to 10 nm, which is beneficial to generate SERS "hot spots" (Fig. S2C). It was reported that the sputtering time makes some differences to the "hot spots", that is, when the sputtering time prolonged, Au NPs deposited on PDMS/AAO continued to increase, thus produced a mass of "hot spots". Therefore, the deposition time was set as 8 min consistent with previous report [51].

HRP-Au/PDMS/AAO substrate has a large surface area with a strong adsorption force. In the presence of H_2O_2, HRP catalyzed

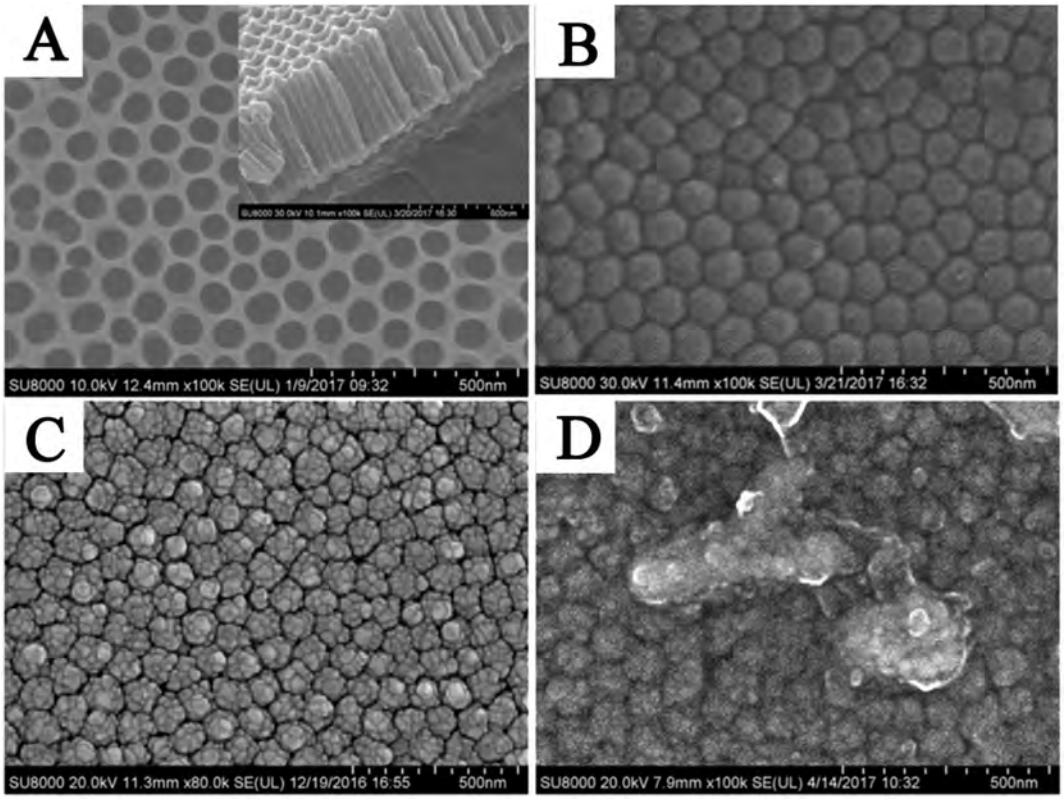

Fig. 1. SEM images of **(A)** AAO (inset, side-view image), **(B)** PDMS/AAO, **(C)** Au/PDMS/AAO and **(D)** MIP-ir-Au/PDMS/AAO.

H_2O_2 and led to the production of these oxidative catalytic states with the formation of acetylacetone radicals, which would induce the polymerization of various of acrylic or vinyl monomers [47,52]. To further verify that HRP has been modified on SERS substrate, the performance of free radical polymerization between immobilized HRP and free HRP, which were carried out in the same concentration of H_2O_2. As shown in Fig. 2A and B, it revealed that both the two methods could initiate the polymerization reaction, and the immobilized HRP (Fig. 2B) could obtain more abundant and uniform polymers than the free HRP (Fig. 2A). From the dynamic light scattering (DLS) measurements in Fig. 2 **C** and Fig. S3, it can further verified that the below polymer has an average size of ~80 nm, and the top one is ~60 nm. The results revealed that the immobilized HRP and free HRP might have a similar reaction process in the presence of H_2O_2. UV–vis spectroscopy was also used to characterize the two polymers (Fig. 2D). It can be seen that the characteristic peak of immobilized HRP showed a slight red-shift compared with the free HRP, which may be ascribed to the space steric hindrance on HRP modified SERS substrate. Through the above characterization, it was demonstrated that the PAT had been successfully adsorbed on the MIP SESR substrate.

3.2. Sensitivity analysis

It is well-known that PAT is a water-soluble unsaturated lactone [53]. Thus solvents with different polarities could have effects on the stability of PAT. Moreover, the pH of solution and incubation time affect the adsorption capacity of MIP-SERS substrate. Therefore, the above effect factors were discussed before in the SERS tests.

Firstly, ten common solvents including water, alcohol, chloroform, methane, DMF, DMSO, acetone, hexane, cyclohexane and toluene were discussed to choose the optimal solvent for PAT (Fig. S4). The results showed that PAT in aqueous solution had the most vigorous SERS intensity at 1205 cm^{-1}, which is the same as previous report [53]. Furthermore, the experiments showed the highest SERS intensity when pH is 5 and incubation time is 1 h (Fig. S5). Thus, the following experiments are performed under the above optimal conditions.

Since the combination of NIP-SERS substrate and PAT mainly depends on physical adsorption, which showed a weak binding force. Besides, PAT was effortlessly washed away during the washing process. Therefore, NIP-SERS substrate behaved a relatively low Raman intensity at the characteristic peak of 1205 cm^{-1} (Fig. 3B). Even when the concentration of PAT reached 10^{-6} M, the SERS intensity is weak (~450). However, for the MIP-SERS substrate, the Raman intensity behaved a noticeable enhancement when PAT is 10^{-6} M (~1700) (Fig. 3A), which revealed the excellent performance of the MIP-SERS substrate. Moreover, the SERS intensity at 1205 cm^{-1} increased gradually as the concentration of PAT increased.

Fig. 3C presented the plots of SERS intensity versus the concentration of PAT at 1205 cm^{-1}. It can be observed that the MIP-SERS substrate can perform qualitative detection of PAT with the range from 10^{-12} to 10^{-5} M. Besides, it behaved a linear relationship between the SERS intensity and PAT concentration of 5×10^{-10} to 10^{-6} M. The linear relationship can be put as $y = 3968.95 + 381.20\,x$ ($R^2 = 0.9962$), where y is the SRES intensity at 1205 cm^{-1} and x is the logarithm value of PAT concentration. The limit of detection (LOD) of MIP-SERS for PAT was calculated to be 8.5×10^{-11} M (S/N = 3, LOD defined by the International Union of Pure and Applied Chemistry) [54]. The low LOD can be ascribed to the specific polymer of MIP and surface-enhanced Raman signal of Au/PDMS/AAO substrate.

Moreover, for NIP-SERS substrate, when the PAT concentration was 0.1 nM, the SERS band at 1205 cm^{-1} is very weak and the

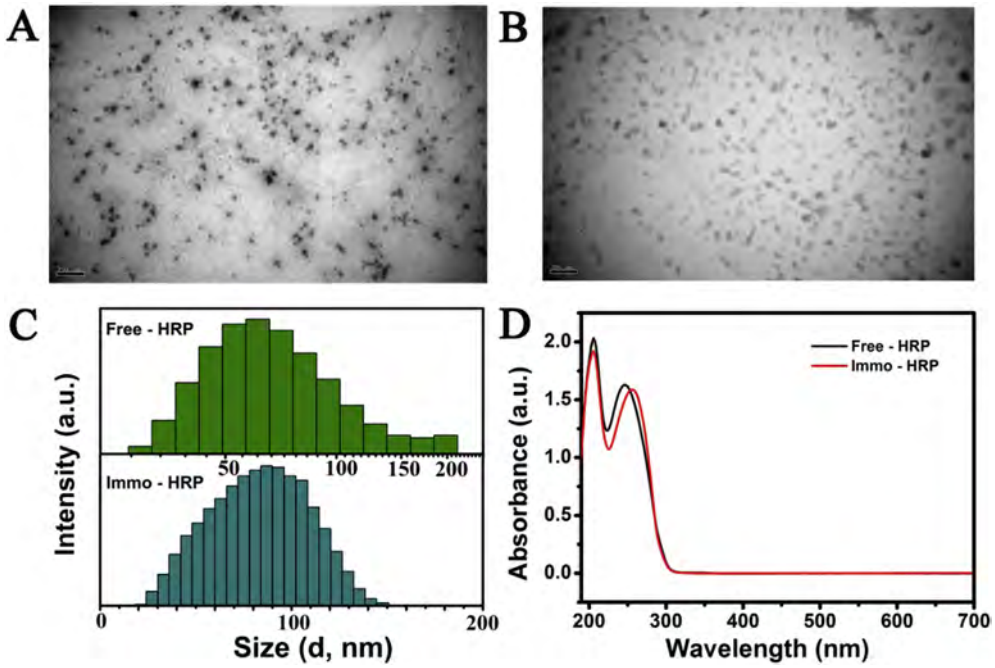

Fig. 2. TEM images of MIPs synthesized by **(A)** free HRP and **(B)** immobilized HRP **(C)** the dynamic light scattering (DLS) measurements of the free HRP (top) and the immobilized HRP (below) **(D)** UV–vis absorption of the two kinds of HRP corresponding to **(A)** and **(B)**.

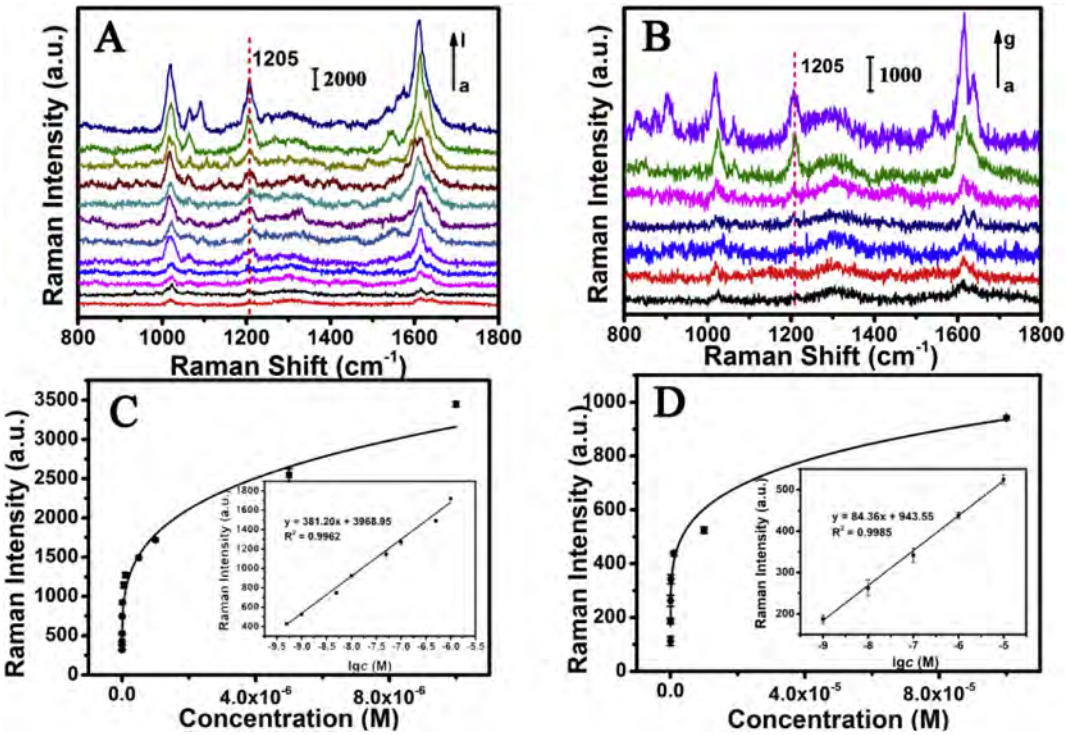

Fig. 3. (**A**) SERS spectra of MIP-SERS substrate (from a to l: 10^{-12} to 10^{-5} M) **(B)** NIP-SERS substrate incubated with different concentrations of PAT (from a to g: 10^{-10} to 10^{-4} M). Plots of SERS intensity at 1205 cm^{-1} *vs* different concentrations of PAT based on **(C)** MIP-SERS substrate (5×10^{-10} to 10^{-6} M) and **(D)** NIP-SERS substrate (10^{-9} to 10^{-5} M). The error bars represent the average standard deviation with three parallel SERS tests.

Raman spectrum is unstable (Fig. 3D), which is consistent with the fact that the interaction force between the NIP-SERS and PAT is non-specific adsorption. Similarly, the inset in Fig. 3D showed the relationship between SERS intensity and PAT concentration of 10^{-9} to 10^{-5} M, which can be put as $y = 943.55 + 84.36$ x ($R^2 = 0.9985$), where y is the SRES intensity and x is the logarithm value of PAT concentration. The LOD of NIP-SERS for PAT was calculated to be 3.6×10^{-9} M (S/N = 3). From what has been discussed above, it indicated that the MIP-SERS substrate exhibited higher sensitivity for PAT. Furthermore, the proposed MIP-SERS method was

compared and listed in Table S1, which revealed that the proposed method owned a higher sensitivity and wider detection range [55].

3.3. Specificity analysis

To verify the specificity of the proposed method, two structural analogues of 5-HMF and oxindole were selected as a control sample (Fig. 4A). As shown in Fig. 4B, the solid samples of 5- HMF and oxindole do not have Raman scattering peaks at 1205 cm^{-1} while PAT has characteristic peaks. Therefore, it is reasonable that the SERS bands at 1205 cm^{-1} was chosen as the indicator for qualitative and quantitative detection of PAT. Moreover, the specificity results revealed that MIP-SERS substrate showed higher sensitivity to PAT than that of NIP-SERS substrate. However, little difference can be observed between the two SERS substrates for the detection of 5-HMF and oxindole, and the Raman intensity is nearly the same as PAT detection with NIP-SERS substrate (Fig. 4C), which indicated that MIP-SERS substrate has a good selectivity to PAT.

To further demonstrate the specificity of the substrate, different concentration ratios of PAT/5-HMF/oxindole mixture were incubated with the substrates and measured by SERS. As depicted in Fig. 4D, the Raman intensity decreases gradually as the concentration ratios of 5-HMF and oxindole increased. For MIP-SERS substrate, when the concentration ratio is $1:10^3:10^3$, the SERS intensity at 1205 cm^{-1} reduced to 48% while decreased to 38% for NIP-SERS substrate. However, even if concentration ratio of PAT is meagre, the SERS intensity of MIP-SERS substrate is higher than NIP-SERS substrate, indicating that MIP-SERS substrate has a higher recognition force. Hence, the above results demonstrated that MIP-SERS substrate has higher selectivity and affinity for PAT, which can be ascribed to the specific role of the imprinted template hole for PAT.

3.4. Repeatability and stability tests

To discuss the reproducibility of as-prepared MIP-SERS substrate, five different batches of substrates were selected randomly to perform the SERS measurement for PAT, which exhibited no noticeable fluctuation in SERS intensity (Fig. 5A). To further prove the repeatability of the MIP-SERS substrate , the SERS signals from five different batches of MIP-SERS substrates were evaluated. And the relative standard deviation (RSD) of the Raman intensity at 1205 cm^{-1} was ~4.7% through statistical calculation (Fig. 5B), which indicated that the MIP-SERS substrate exhibited acceptable reproducibility.

Besides, we choose MIP-SERS substrate randomly and storing it in the air for a month to study the stability of MIP-SERS substrate. As shown in Fig. 5C, the SERS intensity of MIP-SERS substrate showed a relatively minor variation with time increased. The SERS substrate still worked well and the Raman intensity at 1205 cm^{-1} only reduced 30% compared to the initial intensity after 30 days (Fig. 5D), indicating the MIP-SERS substrate behaved excellent SERS enhancement and stability. Judging from the above results, it can verify that MIP-SERS substrate owned excellent repeatability and stability.

3.5. The detection of real sample

Blueberry jam, grapefruit jam and orange juice were selected as real samples to verify the practical application of the SERS substrate. Specifically, blueberry jam, grapefruit jam and orange juice samples were obtained from a local market, which were found no PAT by HPLC and SERS. After adding PAT to the samples, the SERS results were compared with HPLC to evaluate the MIP-SERS substrate. Herein, HPLC test was considered as a standard method by default. As shown in Table 1, both HPLC and SERS showed response to PAT after PAT addition, which indicated that PAT existed in added samples. Specifically, the PAT measured by SERS in blueberry sauce, grapefruit sauce and orange juice real samples were average value with three parallel SERS tests as shown in Fig. S6, and all value of RSD were calculated as shown in Table 1. Moreover, the results showed variations from 96.43% to 112.83% for SERS compared with those of 98.92%–104.66% for HPLC, which suggested that the proposed MIP-SERS substrate behaved acceptable accuracy and sensitivity for the detection of PAT in real samples.

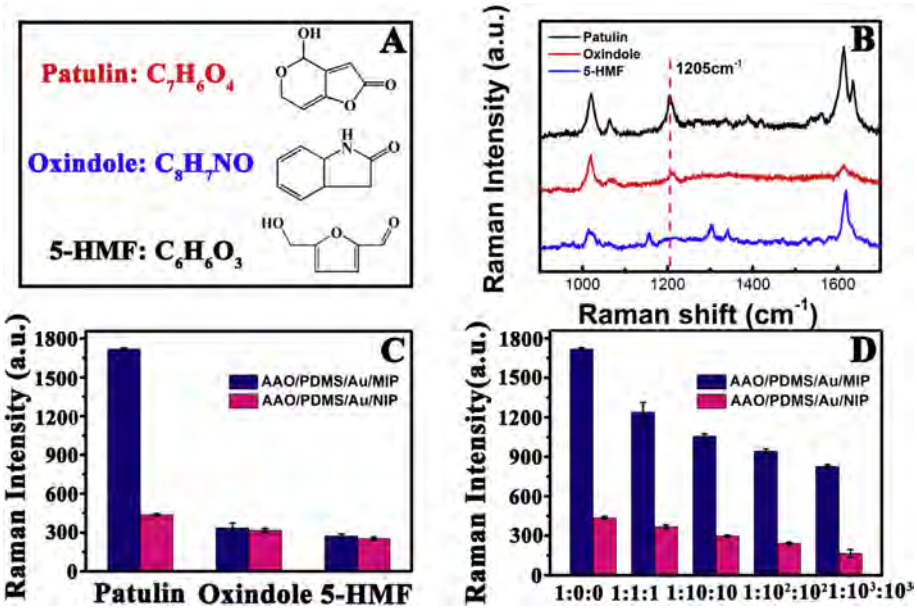

Fig. 4. **(A)** Chemical structures of PAT and the structural analogues (oxindole and 5-HMF). **(B)** Raman spectra of Patulin, Oxindole and 5-HMF. **(C)** The SERS intensity depends on the band at 1205 cm^{-1} for MIP- SERS substrate and NIP-SERS substrate after incubating with Patulin (0.33 μM), oxindole (5 μM) and 5-HMF (5 μM). **(D)** Verification of the selectivity of MIP-SERS and NIP-SERS substrate for PAT (0.33 μM) in the presence of different concentration ratios of $C_{Patulin}/C_{Oxindole}/C_{5\text{-}HMF}$ mixture (1:0:0, 1:1:1, 1:10:10, $1:10^2:10^2$ and $1:10^3:10^3$).

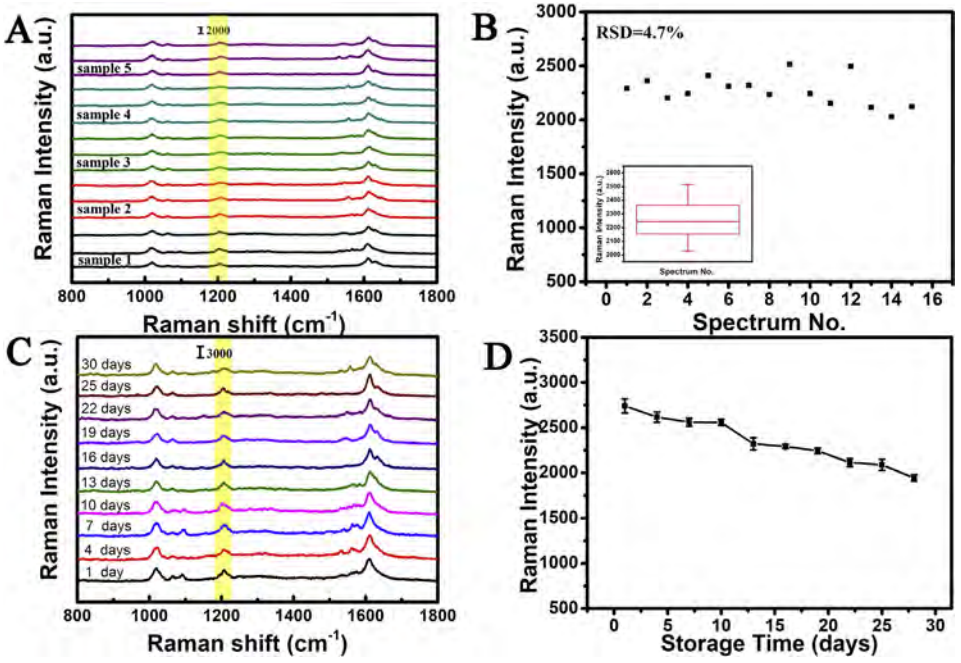

Fig. 5. **(A)** SERS spectra of PAT collected from five MIP-SERS substrates and **(B)** the SERS intensity distribution at 1205 cm^{-1} corresponding to **(A)** (RSD = 4.7%, with three parallel SERS tests). **(C)** SERS spectra of MIP-SERS substrate stored in an air atmosphere at different days (1, 4, 7, 10, 13, 16, 19, 22, 25 and 30 days) and **(D)** the SERS intensity at 1205 cm^{-1} corresponding to **(C)**.

Table 1
Results of PAT detection based on HPLC and SERS methods in real samples. (unit: nM, not found:).

Samples	Detected	Added	Found by HPLC	Recovery	Found by SERS	RSD	Recovery
Blueberry Jam	–	130	136.06	104.66%	146.68	7.3%	112.83%
	–	350	351.93	100.55%	346.37	5.0%	98.96%
Grapefruit Jam	–	130	135.54	104.26%	126.07	8.1%	96.97%
	–	350	362.25	103.50%	337.50	7.2%	96.43%
Orange Juice	–	130	128.60	98.92%	132.15	5.4%	101.65%
	–	350	359.27	102.65%	377.96	4.8%	107.99%

4. Conclusion

In this work, a new type of MIP-ir-Au/PDMS/AAO (MIP-SERS) substrate was synthesized for the label-free detection of PAT. Based on the HRP enzyme initiated in situ polymerization of PAT on Au/PDMS/AAO substrate, the MIP-SERS substrate behaved good selectivity and high sensitivity. The results revealed that the proposed method owned a linear range from 5×10^{-10} to 10^{-6} M with the limit of detection (LOD) of 8.5×10^{-11} M (S/N = 3) for PAT. The proposed method also exhibited acceptable reproducibility (relative standard deviation, RSD = 4.7%), good stability (Raman intensity is above 80% after two weeks) and recoveries from 96.43% to 112.83% with the average RSD of 6.3%.

Moreover, when PAT was mixed with the interferences of 5-HMF and oxindole, MIP-SERS substrate behaved good selectivity for PAT. What is more, owing to the solid-phase interface of the substrate, the method can make the operations more straightforward and more convenient in the sample pretreatment process. Overall, this work provides a new method for the selective and sensitive detection of PAT, which showed great potential in the rapid detection of biotoxin in food samples.

Author contributions

Y. Zhu, L. Wu, and H. Han conceived and designed the experiments. Y. Zhu, W. Yin and H. Yan performed the experiments. Y. Zhu, L. Wu, H. Yan and Z. Lu analysed the results. Y. Zhu, L. Wu and Z. Lu wrote the manuscript. H. Han supervised the entire project.

Declaration of competing interest

The authors declare that they have no known competing financial interests or personal relationships that could have appeared to influence the work reported in this paper.

Acknowledgments

We are very grateful to the financial support from the National Natural Science Foundation of China (21778020), Hubei Provincial Institute for Food Supervision and Test (201601012), Sci-tech Innovation Foundation of Huazhong Agriculture University (2662017PY042, 2662018PY024). Key Laboratory of Guangxi Colleges and Universities for Food Safety and Pharmaceutical Analytical, Item number FPAC2017-ZD-01.

Appendix A. Supplementary data

Supplementary data to this article can be found online at https://doi.org/10.1016/j.aca.2019.12.030

References

[1] S. Wu, N. Duan, W. Zhang, S. Zhao, Z. Wang, Screening and development of DNA aptamers as capture probes for colorimetric detection of patulin, Anal. Biochem. 508 (2016) 58–64.

[2] M. Moake, O. Padilla-Zakour, R. Worobo, Comprehensive review of patulin control methods in foods, Compr. Rev. Food Sci. Food Saf. 4 (2005) 8–21.

[3] D.M. Schumacher, C. Muller, M. Metzler, L. Lehmann, DNA-DNA cross-links contribute to the mutagenic potential of the mycotoxin patulin, Toxicol. Lett. 166 (2006) 268–275.

[4] E. Diao, H. Hou, W. Hu, H. Dong, X. Li, Removing and detoxifying methods of patulin: a review, Trends Food Sci. Technol. 81 (2018) 139–145.

[5] W. Guo, F. Pi, H. Zhang, J. Sun, Y. Zhang, X. Sun, A novel molecularly imprinted electrochemical sensor modified with carbon dots, chitosan, gold nanoparticles for the determination of patulin, Biosens. Bioelectron. 98 (2017) 299–304.

[6] Codex Alimentarius Commission, Code of practice for the prevention and reduction of patulin contamination in apple juice and apple juice ingredients in other beverages, CAC/RPC 50 (2003) 1–6.

[7] X. Li, H. Li, W. Ma, Z. Guo, X. Li, X. Li, Q. Zhang, Determination of patulin in apple juice by single-drop liquid-liquid-liquid microextraction coupled with liquid chromatography-mass spectrometry, Food Chem. 257 (2018) 1–6.

[8] A. Majid Cheraghali, H. Reza Mohammadi, M. Amirahmadi, H. Yazdanpanah, G. Abouhossain, F. Zamanian, M.G. Khansari, M. Afshar, Incidence of patulin contamination in apple juice produced in Iran, Food Control 16 (2005) 165–167.

[9] J.E. Welke, M. Hoeltz, H.A. Dottori, I.B. Noll, Quantitative analysis of patulin in apple juice by thin-layer chromatography using a charge coupled device detector, Food Addit. Contam. A 26 (2009) 754–758.

[10] S.C. Cunha, M.A. Faria, J.O. Fernandes, Determination of patulin in apple and quince products by GC–MS using $^{13}C_{5-7}$ patulin as internal standard, Food Chem. 115 (2009) 352–359.

[11] Y. Yang, Q. Li, G. Fang, S. Wang, Preparation and evaluation of novel surface molecularly imprinted polymers by sol–gel process for online solid-phase extraction coupled with high performance liquid chromatography to detect trace patulin in fruit derived products, RSC Adv. 6 (2016) 54510–54517.

[12] Y. Yang, Y. Yang, B. Shao, J. Zhang, A simple and rapid method for determination of patulin in juice by high performance liquid chromatography tandem mass spectrometry, Food Analytical Methods 10 (2017) 2913–2918.

[13] A. Marsol-Vall, M. Balcells, J. Eras, R. Canela-Garayoa, A rapid gas chromatographic injection-port derivatization method for the tandem mass spectrometric determination of patulin and 5-hydroxymethylfurfural in fruit juices, J. Chromatogr., A 1453 (2016) 99–104.

[14] N. Kharandi, M. Babri, J. Azad, A novel method for determination of patulin in apple juices by GC-MS, Food Chem. 141 (2013) 1619–1623.

[15] L. Wu, G. Li, X. Xu, L. Zhu, R. Huang, X. Chen, Application of nano-ELISA in food analysis: recent advances and challenges, TrAC Trends Anal. Chem. (Reference Ed.) 113 (2019) 140–156.

[16] R. Funari, B. Della Ventura, R. Carrieri, L. Morra, E. Lahoz, F. Gesuele, et al., Detection of parathion and patulin by quartz-crystal microbalance functionalized by the photonics immobilization technique, Biosens. Bioelectron. 67 (2015) 224–229.

[17] A. Pennacchio, A. Varriale, M.G. Esposito, M. Staiano, S. D'Auria, A near-infrared fluorescence assay method to detect patulin in food, Anal. Biochem. 481 (2015) 55–59.

[18] L. Wu, J. Deng, X. Tan, W. Yin, F. Ding, H. Han, Ratiometric fluorescence sensor for the sensitive detection of Bacillus thuringiensis transgenic sequence based on silica coated supermagnetic nanoparticles and quantum dots, Sens. Actuators, B 254 (2018) 206–213.

[19] L. Wu, X. Xiao, K. Chen, W. Yin, Q. Li, P. Wang, Z. Lu, J. Ma, H. Han, Ultrasensitive SERS detection of Bacillus thuringiensis special gene based on Au@Ag NRs and magnetic beads, Biosens. Bioelectron. 92 (2017) 321–327.

[20] K. Kneipp, Y. Wang, H. Kneipp, L.T. Perelman, I. Itzkan, R.R. Dasari, M.S. Feld, Single molecule detection using surface-enhanced Raman scattering (SERS), Phys. Rev. Lett. 78 (1997) 1667–1670.

[21] S. Nie, S.R. Emory, Probing single molecules and single nanoparticles by surface-enhanced Raman scattering, Science 275 (1997) 1102–1106.

[22] M. Sackmann, A. Materny, Surface enhanced Raman scattering (SERS)-aquantitative analytical tool? J. Raman Spectrosc. 37 (2006) 305–310.

[23] W. Shen, X. Lin, C. Jiang, C. Li, H. Lin, J. Huang, S. Wang, G. Liu, X. Yan, Q. Zhong, B. Ren, Reliable Quantitative SERS analysis facilitated by core-shell nanoparticles with embedded internal standards, Angew. Chem., Int. Ed. Engl. 54 (2015) 7308–7312.

[24] W.E. Smith, Practical understanding and use of surface enhanced Raman scattering/surface enhanced resonance Raman scattering in chemical and biological analysis, Chem. Soc. Rev. 37 (2008) 955–964.

[25] S. Kasera, F. Biedermann, J.J. Baumberg, O.A. Scherman, S. Mahajan, Quantitative SERS using the sequestration of small molecules inside precise plasmonic nanoconstructs, Nano Lett. 12 (2012) 5924–5928.

[26] R. Hu, R. Tang, J. Xu, F. Lu, Chemical nanosensors based on molecularly-imprinted polymers doped with silver nanoparticles for the rapid detection of caffeine in wastewater, Anal. Chim. Acta 1034 (2018) 176–183.

[27] A. Bossi, F. Bonini, A.P. Turner, S.A. Piletsky, Molecularly imprinted polymers for the recognition of proteins: the state of the art, Biosens. Bioelectron. 22 (2007) 1131–1137.

[28] E.M. Dursun, R. Üzek, N. Bereli, S. Şenel, A. Denizli, Synthesis of novel monolithic cartridges with specific recognition sites for extraction of melamine, React. Funct. Polym. 109 (2016) 33–41.

[29] P. Lulinski, Molecularly imprinted polymers based drug delivery devices: a way to application in modern pharmacotherapy, A review, Mater. Sci. Eng. 76 (2017) 1344–1353.

[30] M. Jia, Z. Zhang, J. Li, X. Ma, L. Chen, X. Yang, Molecular imprinting technology for microorganism analysis, TrAC Trends Anal. Chem. (Reference Ed.) 106 (2018) 190–201.

[31] R. Li, Y. Feng, G. Pan, L. Liu, Advances in molecularly imprinting technology for bioanalytical applications, Sensors 19 (2019) 177.

[32] X. Ying, H.-T. Yoshioka, C. Liu, F. Sassa, K. Hayashi, Molecular imprinting technique in putrescine visualized detection, Sens. Actuators, B 258 (2018) 870–880.

[33] W. Yin, L. Wu, F. Ding, Q. Li, P. Wang, J. Li, Z. Lu, H. Han, Surface-imprinted SiO2@Ag nanoparticles for the selective detection of BPA using surface enhanced Raman scattering, Sens. Actuators, B 258 (2018) 566–573.

[34] L. Chang, Y. Ding, X. Li, Surface molecular imprinting onto silver microspheres for surface enhanced Raman scattering applications, Biosens. Bioelectron. 50 (2013) 106–110.

[35] E.L. Holthoff, D.N. Stratis-Cullum, M.E. HankusA, Nanosensor for TNT detection based on molecularly imprinted polymers and surface enhanced Raman scattering, Sensors 11 (2011) 2700–2714.

[36] H. Li, X. Wang, Z. Wang, Y. Wang, J. Dai1, L. Gao, M. Wei, Y. Yan, C. Li, A polydopamine-based molecularly imprinted polymer on nanoparticles of type SiO2@rGO@Ag for the detection of λ-cyhalothrin via SERS, Microchimica Acta 185 (2018) 193.

[37] M. Shen, N. Duan, S. Wu, Y. Zou, Z. Wang, Polydimethylsiloxane gold nanoparticle composite film as structure for aptamer-based detection of Vibrio parahaemolyticus by surface-enhanced Raman spectroscopy, Food Analytical Methods 12 (2019) 595–603.

[38] W. Koetniyom, P. Somboonsaksri, S. Kalasung, C. Chananonnawathorn, V. Patthanasettakul, M. Horprathum, N. Nuntawong, S. Limwichean, P. Eiamchai, The fabrication of PDMS polymer templates on aluminum sheet by laser marking in micro-nano structure scale for surface-enhanced Raman spectroscopy (SERS), in: AIP Conference Proceedings, AIP Conference Proceedings, 2018, 2010.

[39] M. Villegas, Z. Cetinic, A. Shakeri, T.F. Didar, Fabricating smooth PDMS microfluidic channels from low-resolution 3D printed molds using an omniphobic lubricant-infused coating, Anal. Chim. Acta 1000 (2018) 248–255.

[40] M. Tanyeri, S. Tay, Viable cell culture in PDMS-based microfluidic devices, Methods Cell Biol. 148 (2018) 3–33.

[41] R. Thuenauer, S. Nicklaus, M. Frensch, K. Troendle, J. Madl, W. Romer, A microfluidic biochip for locally confined stimulation of cells within an epithelial monolayer, RSC Adv. 8 (2018) 7839–7846.

[42] E. Valera, J. Berger, U. Hassan, T. Ghonge, J. Liu, M. Rappleye, J. Winter, D. Abboud, Z. Haidry, R. Healey, N. Hung, N. Leung, N. Mansury, A. Hasnain, C. Lannon, Z. Price, K. White, R. Bashir, A microfluidic biochip platform for electrical quantification of proteins, Lab Chip 18 (2018) 1461–1470.

[43] P. Wang, L. Wu, Z. Lu, Q. Li, W. Yin, F. Ding, et al., Gecko-inspired nanotentacle surface-enhanced Raman spectroscopy substrate for sampling and reliable detection of pesticide residues in fruits and vegetables, Anal. Chem. 89 (2017) 2424–2431.

[44] H. Masuda, K. Fukuda, Ordered metal nanohole arrays made by a two-step replication of honeycomb structures of anodic alumina, Sciences 268 (1995) 1466–1468.

[45] T. Kim, S. Jeong, Highly ordered anodic alumina nanotemplate with about 14 nm diameter, Korean J. Chem. Eng. 25 (2008) 609–611.

[46] J. Zhao, Y. Zhang, H. Li, Y. Wen, X. Fan, F. Lin, L. Tan, S. Yao, Ultrasensitive electrochemical aptasensor for thrombin based on the amplification of aptamer-AuNPs-HRP conjugates, Biosens. Bioelectron. 26 (2011) 2297–2303.

[47] M. Daoud Attieh, Y. Zhao, A. Elkak, A. Falcimaigne-Cordin, K. Haupt, Enzyme-initiated free-radical polymerization of molecularly imprinted polymer nanogels on a solid phase with an immobilized radical source, Angew. Chem. 56 (2017) 3339–3343.

[48] F. Shao, Z. Lu, C. Liu, H. Han, K. Chen, W. Li, Q. He, H. Peng, J. Chen, Hierarchical nanogaps within bioscaffold arrays as a high-performance SERS substrate for animal virus biosensing, Appl. Mater. Interfaces. 6 (2014) 6281–6289.

[49] M. Copel, M. Reuter, E. Kaxiras, R. Tromp, Surfactants in epitaxial growth, Phys. Rev. Lett. 63 (1989) 632.

[50] J. Floro, S. Hearne, J. Hunter, P. Kotula, E. Chason, S. Seel, C. Thompson, The dynamic competition between stress generation and relaxation mechanisms during coalescence of Volmer–Weber thin films, J. Appl. Phys. 89 (2001) 4886–4897.

[51] J. Li, H. Yan, X. Tan, Z. Lu, H. Han, Cauliflower-inspired 3D SERS substrate for multiple mycotoxins detection, Anal. Chem. 91 (2019) 3885–3892.

[52] T. Su, D. Zhang, Z. Tang, Q. Wu, Q. Wang, HRP-mediated polymerization forms tough nanocomposite hydrogels with high biocatalytic performance, Chem. Commun. 49 (2013) 8033–8035.

[53] M. de Champdore, P. Bazzicalupo, L. de Napoli, D. Montesarchio, G. Fabio, I. Cocozza, A. Parracino, M.' Rossi, S. D'Auria, A new competitive fluorescence assay for the detection of patulin toxin, Anal. Chem. 79 (2007) 751–757.
[54] IUPAC Compendium of Chemical Terminology the"Gold Book", second ed., Blackwell Scientific Publications, Oxford, 1997.
[55] K. Danzer, International union of pure and applied chemistry guidelines for calibration in analytical chemistry: fundamentals and single component calibration. Pure Appl. Chem. 70(4) 993-1014.